

Kunda, NK, Alfagih, IM, Dennison, SR, Somavarapu, S, Merchant, Z, Hutcheon, GA and Saleem, IY

Dry powder pulmonary delivery of cationic PGA-co-PDL nanoparticles with surface adsorbed model protein

<https://researchonline.ljmu.ac.uk/id/eprint/1890/>

Article

Citation (please note it is advisable to refer to the publisher's version if you intend to cite from this work)

Kunda, NK, Alfagih, IM, Dennison, SR, Somavarapu, S, Merchant, Z, Hutcheon, GA and Saleem, IY (2015) Dry powder pulmonary delivery of cationic PGA-co-PDL nanoparticles with surface adsorbed model protein. International Journal of Pharmaceutics. 492 (1-2). pp. 213-222. ISSN 0378-

LJMU has developed **LJMU Research Online** for users to access the research output of the University more effectively. Copyright © and Moral Rights for the papers on this site are retained by the individual authors and/or other copyright owners. Users may download and/or print one copy of any article(s) in LJMU Research Online to facilitate their private study or for non-commercial research. You may not engage in further distribution of the material or use it for any profit-making activities or any commercial gain.

The version presented here may differ from the published version or from the version of the record. Please see the repository URL above for details on accessing the published version and note that access may require a subscription.

For more information please contact researchonline@ljmu.ac.uk

Dear Author,

Please, note that changes made to the HTML content will be added to the article before publication, but are not reflected in this PDF.

Note also that this file should not be used for submitting corrections.



Contents lists available at ScienceDirect

International Journal of Pharmaceutics

journal homepage: www.elsevier.com/locate/ijpharm



Dry powder pulmonary delivery of cationic PGA-co-PDL nanoparticles with surface adsorbed model protein

Nitesh K. Kunda^a, Iman M. Alfagih^{a,b}, Sarah R. Dennison^c, Satyanarayana Somavarapu^d, Zahra Merchant^d, Gillian A. Hutcheon^a, Imran Y. Saleem^{a,*}

^a Formulation and Drug Delivery Research, School of Pharmacy and Biomolecular Sciences, Liverpool John Moores University, Liverpool, United Kingdom

^b Department of Pharmaceutics, College of Pharmacy, King Saud University, Saudi Arabia

^c Research and Innovation, University of Central Lancashire, Preston, United Kingdom

^d Department of Pharmaceutics, School of Pharmacy, University College London, London, United Kingdom

ARTICLE INFO

Article history:

Received 18 May 2015

Received in revised form 2 July 2015

Accepted 6 July 2015

Available online xxx

Keywords:

Dry powder inhalation

Nanoparticles

Pulmonary delivery

Spray drying

Proteins

ABSTRACT

Pulmonary delivery of macromolecules has been the focus of attention as an alternate route of delivery with benefits such as; large surface area, thin alveolar epithelium, rapid absorption and extensive vasculature. In this study, a model protein, bovine serum albumin (BSA) was adsorbed onto cationic PGA-co-PDL polymeric nanoparticles (NPs) prepared by a single emulsion solvent evaporation method using a cationic surfactant didodecyldimethylammonium bromide (DMAB) at 2% w/w (particle size: 128.64 ± 06.01 nm and zeta-potential: $+42.32 \pm 02.70$ mV). The optimum cationic NPs were then surface adsorbed with BSA, NP:BSA (100:4) ratio yielded 10.01 ± 1.19 μ g of BSA per mg of NPs. The BSA adsorbed NPs (5 mg/ml) were then spray-dried in an aqueous suspension of L-leucine (7.5 mg/ml, corresponding to a ratio of 1:1.5/NP:L-leu) using a Büchi-290 mini-spray dryer to produce nanocomposite microparticles (NCMPs) containing cationic NPs. The aerosol properties showed a fine particle fraction (FPF, $d_{ae} < 4.46$ μ m) of $70.67 \pm 4.07\%$ and mass median aerodynamic diameter (MMAD) of 2.80 ± 0.21 μ m suggesting a deposition in the respiratory bronchiolar region of the lungs. The cell viability was $75.76 \pm 03.55\%$ (A549 cell line) at 156.25 μ g/ml concentration after 24 h exposure. SDS-PAGE and circular dichroism (CD) confirmed that the primary and secondary structure of the released BSA was maintained. Moreover, the released BSA showed $78.76 \pm 1.54\%$ relative esterolytic activity compared to standard BSA.

© 2015 Published by Elsevier B.V.

1. Introduction

An increase in mortality and morbidity associated with pulmonary diseases has led to the exploration of pulmonary drug delivery as a non-invasive approach for the treatment and management of these diseases and also for administration of therapeutics for systemic delivery (Carlotta et al., 2011; Yang et al., 2008). The lung as a delivery route offers a large surface area (80–90 sq m), extensive vasculature, a thin alveolar epithelium (0.1–0.5 μ m) leading to rapid absorption (Scheuch et al., 2006). It is also

believed that compared to any other entry portal in the body, the pulmonary epithelia appears to be more permeable to macromolecules (Patton, 1996). Advancements in biotechnology in the last decade have led to the development of new therapeutics such as peptides, proteins and other macromolecules (Sullivan et al., 2006). Despite barriers such as the respiratory mucus, mucociliary clearance, macrophages, enzymes and basement membrane that limit absorption (Agu et al., 2001), several macromolecules have been extensively investigated such as insulin (Al-Qadi et al., 2012; Kling, 2014), bovine serum albumin (BSA) (Jiang et al., 2010; Kunda et al., 2014), calcitonin (Yamamoto et al., 2005) for delivery via the pulmonary route.

Biodegradable nanoparticles (NPs), are being explored for the delivery of macromolecules as they offer improved bioavailability, controlled or sustained release and biocompatibility (Kumari et al., 2010; Tawfeek et al., 2011). Several factors such as polymer properties, size and charge of NPs, and the stabilizer(s) employed in the preparation of NPs play a vital role in determining their uptake, biodistribution, drug loading and fate after administration,

Abbreviations: BSA, bovine serum albumin; CD, circular dichroism; DMAB, didodecyldimethylammonium bromide; L-leu, L-leucine; NPs, nanoparticles; NCMPs, nanocomposite microparticles; PGA-co-PDL, poly(glycerol adipate-co- ω -pentadecalactone); PVA, polyvinyl alcohol; SD, spray-drying; SDS-PAGE, sodium dodecyl sulfate-polyacrylamide gel electrophoresis.

* Corresponding author at: Liverpool John Moores University, School of Pharmacy and Biomolecular Sciences, Byrom Street, Liverpool, L3 3AF, United Kingdom.
Fax: +44 151 231 2265.

E-mail address: I.Saleem@ljmu.ac.uk (I.Y. Saleem).

<http://dx.doi.org/10.1016/j.ijpharm.2015.07.015>

0378-5173/© 2015 Published by Elsevier B.V.

all of which affect the therapeutic efficacy (Bhardwaj et al., 2009; Peetla and Labhasetwar, 2009). Herein, we used a cationic surfactant, quaternary ammonium salt didodecyl dimethyl ammonium bromide (DMAB) to produce positively charged NPs. It is established that the cationic surfactant DMAB produces small, stable NPs and prevents particle agglomeration (Bhardwaj et al., 2009; Chen et al., 2010; Hariharan et al., 2006; Kwon et al., 2001). The particle size and surface charge of NPs are known to play an important role in determining the cellular uptake, and cationic NPs compared to anionic NPs (negatively charged) or neutral NPs, have better interactions with the negatively charged cell membrane thereby improving their cellular uptake (Hariharan et al., 2006; Peetla and Labhasetwar, 2009). NPs and protein can be attached together either by simple physical adsorption based on charge or hydrophobic interactions (Mody et al., 2013; Wendorf et al., 2006), or complex processes; such as chemical conjugation and encapsulation (Zhao et al., 2014). The encapsulation of proteins may present some problems such as low loading and loss of protein activity due to harsh formulation conditions; such as interaction with organic solvents and the higher stirring speed employed in the NP preparation process (Bramwell and Perrie, 2006; Jiang et al., 2005). Alternatively, an adsorption process avoids protein contact with the harsh conditions offering enhanced stability over encapsulated proteins hence providing a promising alternative for encapsulation (Bramwell and Perrie, 2006; Florindo et al., 2010).

Due to their small size and low inertia NPs are exhaled after inhalation resulting in low doses in the lungs, and the high surface energy promotes aggregation making them difficult to handle (Stevanovic and Uskokovic, 2009; Yang et al., 2008). Therefore, the NPs to be used in pulmonary delivery are required to be formulated into microcarriers for ideal aerosolisation properties (Sinsuebpol et al., 2013). This can be achieved using excipients, such as lactose, mannitol, trehalose and L-leucine (L-leu) to produce nanocomposite microparticles (NCMPs) that encompass NPs in a microcarrier (Li et al., 2005; Seville et al., 2007). The NCMPs are formulated using manufacturing techniques such as freeze-drying, spray-drying (SD), spray-freeze drying or supercritical fluid technologies (Al-fagih et al., 2011; Kunda et al., 2013). The aim of this study was to produce cationic NPs with surface adsorbed BSA, and formulate the NPs into NCMPs via SD using L-leu as a carrier for dry powder inhalation.

2. Materials and methods

2.1. Materials

Bovine serum albumin (BSA, MW 67 KDa), didodecyl dimethyl ammonium bromide (DMAB), phosphate buffered saline (PBS, pH 7.4) tablets, poly(vinyl alcohol) (PVA, MW 9–10 K, 80%), RPMI-1640 medium with L-glutamine and NaHCO_3 , thiazoly blue tetrazolium bromide (MTT), tween 80[®] and 4-nitrophenyl acetate were obtained from Sigma–Aldrich, UK. L-leucine (L-leu) was purchased from BioUltra, Sigma, UK. Tissue culture flasks (75 cm²) with vented cap, 96-well flat bottom plates, acetone, acetonitrile (ACN, HPLC grade), antibiotic/antimycotic Solution (100X), dichloromethane (DCM), dimethyl sulfoxide (DMSO) were purchased from Fisher Scientific, UK. Divinyl adipate was obtained from Fluorochem, UK. Fetal calf serum (FCS) heat inactivated was purchased from Biosera UK. Micro BCA[™] protein assay kit was purchased from Thermo Scientific, UK. Poly(glycerol adipate-co- ω -pentadecalactone) (PGA-co-PDL, MW of 14.7 KDa) was synthesized in our laboratory at LJMU as previously published by Thompson et al. (Thompson et al., 2006) and human adenocarcinoma alveolar basal epithelial cell line, A549, was purchased from ATCC.

2.2. Preparation of nanoparticles

The cationic NPs were prepared using a previously established oil-in-water (o/w) single emulsion solvent evaporation method (Kunda et al., 2014). Briefly, PGA-co-PDL, (200 mg), (Nile Red, NR, 0.5 mg for confocal microscopy) and DMAB (0, 1 and 2% w/w of polymer) were dissolved in 2 ml DCM and upon addition to 5 ml of 5% w/v poly(vinyl alcohol) (PVA) was probe sonicated (20 microns amplitude) for 2 min under ice to obtain an emulsion. This was immediately added drop wise to 20 ml of 0.75% w/v PVA under magnetic stirring at a speed of 500 RPM. This mixture was left stirring at room temperature for 3 h to facilitate the evaporation of DCM. The NP suspension was collected using centrifugation (78,000 \times g, 40 min, 4 °C), washing twice to remove unbound and excess surfactant. The NPs were then surface adsorbed with protein as described in Section 2.3.

2.3. Protein adsorption and quantification

The NP suspension (equivalent to 10 mg) was resuspended in 4 ml of BSA (or FITC-BSA for confocal microscopy) at different NP: BSA ratios (100:4–100:20) corresponding to 100–500 $\mu\text{g/ml}$ BSA. After 1 h of rotation at 20 RPM on a HulaMixer[™] Sample Mixer (Life Technologies, Invitrogen, UK) the NP suspensions were centrifuged and the supernatant analysed for protein content using a micro BCA protein assay kit. The amount of BSA adsorbed per milligram of NPs ($n = 3$) was calculated using Eq. (1):

$$\text{Adsorption } (\mu\text{per mg of NPs}) = \frac{(\text{Initial protein conc} - \text{Supernatant protein conc})}{\text{Amount of NPS}} \quad (1)$$

2.4. Characterization of nanoparticles

Morphological analysis of NPs was performed by transmission electron microscopy (TEM) using a FEI Morgagni Transmission Electron Microscope (Philips Electron Optics BV, Netherlands) at an acceleration voltage of 100 kV. Approximately 50 μl of the NP suspension was stained with 2% ammonium molybdate and placed on a carbon coated copper grid. Digital images were taken at magnification of 44,000 and 110,000.

Particle size, poly dispersity index (PDI) and surface charge (zeta potential) were measured by dynamic laser scattering (DLS) using a laser particle size analyser (Zetasizer Nano ZS, Malvern Instruments Ltd., UK). An aliquot of 100 μl of the NP suspension was diluted with 5 ml of deionized water loaded into a cuvette and the measurements recorded at 25 °C ($n = 3$).

2.5. Preparation of nanocomposite microparticles

The NPs were incorporated into NCMPs using L-leu as a carrier at a weight ratio of 1:1.5 (NP:L-leu). The empty NPs, BSA adsorbed NPs or FITC-BSA adsorbed Nile Red NPs (NR NPs for confocal microscopy) were dispersed in distilled water containing L-leu at a concentration of 12.5 mg/ml (5 mg/ml NPs and 7.5 mg/ml L-leu). The resultant suspension was then spray-dried using a Büchi B-290 mini spray-dryer (Büchi Labortechnik, Flawil, Switzerland) at a feed rate of 10%, an atomizing air flow of 400 L/h, aspirator capacity of 100% and an inlet temperature of 100 °C (outlet temperature approximately 45 ± 2 °C). The dry NCMPs were collected from the cyclone (Büchi Labortechnik) and stored in a desiccator at room temperature until further use.

2.6. Characterization of nanocomposite microparticles

2.6.1. Yield, particle size, morphology and moisture content

The yield (% w/w) was calculated as the difference in weight before and after collection to the initial total dry mass ($n=3$)

Particle size and PDI of NPs after re-dispersion of the NCMPs in distilled water were measured to confirm the recovery of NPs from the NCMPs. The measurements were performed as described in Section 2.4, where 5 mg of NCMPs were dispersed in 2 ml of deionized water, loaded into a cuvette and the readings were recorded at 25 °C ($n=3$).

The spray-dried NCMPs were observed under the scanning electron microscope (FEI Quanta™ 200 ESEM, Holland). The samples were mounted onto aluminium pin stubs (13 mm) layered with a sticky conductive carbon tab and coated with palladium (10–15 nm) using a sputter coater (EmiTech K 550X Gold Sputter Coater, 25 mA) before examination under the microscope.

Thermo Gravimetric Analysis (TGA) was used to determine the residual moisture content in the spray-dried NCMPs. Measurements were carried out in triplicate using a TA Instruments TGA Q50, UK equipped with TA Universal Analysis 2000 software. Solid samples (4–15 mg) were loaded on open platinum TGA pan suspended from a microbalance and heated from 25 to 650 °C at 10 °C per min. The moisture content (water loss) was analysed for data collected between 25 and 120 °C.

2.7. Characterization of BSA and nanoparticle association

To visualise the adsorption of BSA onto the NPs, the spray-dried NCMPs containing FITC-BSA adsorbed NR NPs were observed using a Zeiss 510 Meta confocal laser scanning microscope mounted on an Axiovert 200M BP inverted microscope. To obtain confocal images, 1–2 mg of spray-dried NCMPs were placed in a single well of an 8-well chambered slide (Fisher Scientific, UK) and imaged by excitation at a wavelength of 488 nm (green channel for FITC-BSA) and 543 nm (red channel for Nile Red NPs) and with a Plan Neofluar 63 × /0.30 numerical aperture objective lens. The obtained confocal images were then analysed using the Zeiss LSM software.

2.8. In vitro release studies

The NCMPs (20 mg) were weighed into eppendorfs and dispersed in 2 ml of PBS, pH 7.4, and left rotating at a speed of 20 RPM on a HulaMixer™ Sample Mixer (Life Technologies, Invitrogen, UK) for 48 h at 37 °C. The samples were centrifuged (accuSpin Micro 17, Fisher Scientific, UK) at 17,000 × g for 30 min at pre-determined time intervals ranging from 0, 30 min, 1, 2, 4, 6, 20, 24 and 48 h, and 1 ml of the supernatant was removed for analysis and replaced with fresh medium. The supernatant was analysed using the micro BCA protein assay. The percentage cumulative BSA released was calculated using Eq. (2):

$$\% \text{Cumulative BSA released} = \frac{\text{Cumulative BSA released}}{\text{BSA loaded}} \times 100 \quad (2)$$

2.9. Protein stability and activity

2.9.1. Sodium dodecyl sulfate-polyacrylamide gel electrophoresis

Sodium dodecyl sulfate-polyacrylamide gel electrophoresis (SDS-PAGE) was employed to determine the primary structure of BSA. The spray-dried NCMPs, 20 mg, were suspended in 1 ml of 2% SDS in HPLC grade water and were rotated on a HulaMixer™ Sampler Mixer for 48 h. After, the sample was centrifuged (accuSpin Micro 17, Fisher Scientific, UK) at 17,000 × g, 30 min,

the supernatant was collected and stability of BSA determined. The SDS-PAGE was performed on a CVS10D omniPAGE vertical gel electrophoresis system (Geneflow Limited, UK). A 9% stacking gel was prepared using ProtoGel stacking buffer (Geneflow Limited, UK). The protein loading buffer blue (2×) (Geneflow Limited, UK) was added to the samples in 1:1 (v/v) buffer-to-sample ratio. Protein molecular weight markers (10–220 KDa, Geneflow Limited, UK) and BSA were used as controls. 25 µl of sample per well were loaded and the gel was run for approximately 2.5 h at a voltage of 100 V with Tris-Glycine-SDS PAGE buffer (10×) (Geneflow Limited, UK). The gel was stained with colloidal coomassie blue and then destained in distilled water overnight. An image of the gel was scanned on a gel scanner (GS-700 Imaging Densitometer, Bio-Rad) equipped with Quantity One software.

2.9.2. Circular dichroism

Circular dichroism (CD) was employed to study the secondary structure of BSA. The CD spectra of BSA standard (control) and BSA released from NPs after 48 h were collected using a J-815 spectropolarimeter (Jasco, UK) at 20 °C as previously described (Greenfield, 2007). The final spectra was an average of five scans obtained at a scan speed of 50 nm min⁻¹ using a 10 mm path-length cell, 260–180 nm wavelength range with a data pitch of 0.5 nm and band width of 1 nm. The baseline acquired in the absence of sample was subtracted for the spectra of all samples (Henzler Wildman et al., 2003) and the secondary structure then analysed using the CDSSTR method from the DichroWeb server (Whitmore and Wallace, 2004; Whitmore et al., 2010).

2.9.3. BSA activity

The esterolytic activity of BSA was investigated using 4-nitrophenyl acetate esterase substrate as described by Abbate et al. (Abbate et al., 2012). Briefly, 1.2 ml of 50 µg/ml of released BSA from NCMPs (see Section 2.8) in PBS buffer was added to 15 µl of a freshly prepared solution of 5 mM 4-nitrophenyl acetate in ACN and incubated for 1 h using a HulaMixer™ Sample Mixer. After 1 h, the absorbance was measured at 405 nm. Standard BSA (50 µg/ml) and PBS buffer were used as positive and negative controls respectively. The ratio of absorbance between the released BSA and standard BSA was calculated as the relative residual esterolytic activity, with the activity of standard BSA considered to be 100%.

2.10. Determination of the aerosol properties of NCMPs using next generation impactor

The aerosol properties of the spray-dried formulations were determined using a Next Generation Impactor, NGI (Copley Scientific Limited, UK). Four capsules of hydroxypropyl methylcellulose, HPMC, were loaded to contain 12.5 mg of BSA adsorbed cationic NPs/NCMPs spray-dried powder (equivalent to 5 mg of NPs), and placed in a Cyclohaler® (Tevapharma). The samples were drawn into the NGI at a flow rate of 60 l/min for 4 s, and collected using a known volume of 2% SDS in HPLC grade water, and left on a shaker for 48 h for the BSA to be released from the NCMPs. The samples were centrifuged and the amount of BSA deposited was analysed using a micro BCA protein assay kit. The fine particle fraction (FPF, %) was determined as the fraction of emitted dose deposited in the NGI with $d_{ae} < 4.46 \mu\text{m}$, the mass median aerodynamic diameter (MMAD) was calculated from log-probability analysis, and the fine particle dose (FPD) was expressed as the mass of drug deposited in the NGI, $d_{ae} < 4.46 \mu\text{m}$ ($n=3$). In addition, the percentage (%) deposition was calculated as the percentage ratio of the amount of BSA collected in a stage to that of the total amount of BSA collected from all stages.

2.11. Cell viability study

The *in vitro* cytotoxicity of the cationic NPs and NPs/NCMPs was evaluated using the MTT assay. A549 cells were cultured in RPMI-1640/10% fetal calf serum/1% antibiotic/antimycotic medium. 100 μ l (2.5×10^5 cells/ml) of cell suspension were seeded in 96-well plates and placed in an incubator at 37 °C for 24 h supplemented with 5% CO₂. This was followed by the addition of 100 μ l freshly prepared NPs or NPs/NCMP dispersions in medium at various concentrations (0–312.5 μ g/ml) ($n=3$) with 10% dimethyl sulfoxide (DMSO) as a positive control. Following 24 h incubation, 40 μ l of a 5 mg/ml MTT solution in PBS was added to each well and incubated for 2 h at 37 °C. The medium was removed and replaced with DMSO (100 μ l) to dissolve the formazan crystals. The absorbance was measured at 570 nm using a plate reader (Molecular Devices, SpectraMAX 190). The percentage of viable cells in each well was calculated as the absorbance ratio between nanoparticle-treated and untreated control cells.

2.12. Statistical analysis

All statistical analysis was performed using Minitab® 16 Statistical Software and significant differences between formulations were assumed at $p < 0.05$. One-way analysis of variance (ANOVA) with the Tukey's comparison was employed for comparing the formulations with each other. All values are expressed as their Mean \pm SD.

3. Results

3.1. Preparation and characterization of nanoparticles

The addition of a cationic surfactant, DMAB, at 1% w/w to the organic solvent during particle formulation produced no significant difference in particle size and PDI whereas the surface charge changed from negative to positive, as shown in Table 1. Moreover, with an increase in the concentration of DMAB, from 1 to 2% w/w, the particle size of NPs decreased accompanied by an increase in surface charge. However, it was observed that after two washes (centrifugation) the surface charge had decreased with an increase in particle size (Table 1) for all concentrations of DMAB.

The TEM images of NPs indicated that the NPs appeared to be smooth and spherical in shape with no visible aggregation or adhesion between NPs (Fig. 1a & b).

3.2. Protein adsorption and quantification

The average adsorption of BSA onto cationic NPs, as shown in Fig. 2a, significantly increased from a NP:BSA ratio of 100:4 (10.01 ± 1.19 μ g per mg of NPs), 100:7 (33.70 ± 3.25 μ g per mg of NPs), 100:10 (54.04 ± 1.66 μ g per mg of NPs), 100:12 (64.10 ± 4.05 μ g per mg of NPs), 100:16 (79.54 ± 0.57 μ g per mg

of NPs) to 100:20 (91.29 ± 3.66 μ g per mg of NPs) ($p < 0.05$, ANOVA/Tukey's comparison; all values are significantly different to each other).

Table 2 lists the particle size, PDI and zeta-potential of cationic NPs with and without BSA adsorbed. Here, the NPs without BSA adsorption were treated same as the NPs with BSA adsorption, and both these preparations were subjected to three centrifugation steps. An additional centrifugation step was necessitated to remove the unbound BSA after adsorption. The significant increase ($p < 0.05$, ANOVA/Tukey's comparison) in particle size of NPs accompanied with a change in the surface charge was ascribed to the adsorption of BSA onto NPs as confirmed using confocal microscopy (Section 3.4, Fig. 2b).

3.3. Characterization of Nanocomposite Microparticles

3.3.1. Yield, particle size, morphology and moisture content

A reasonable yield of spray drying, $44.82 \pm 4.12\%$ for the empty cationic NPs/NCMPs and $48.00 \pm 5.66\%$ for BSA adsorbed cationic NPs/NCMPs was obtained.

The size of the NPs after dispersion in water for SD empty cationic NPs/NCMPs was 216.50 ± 25.45 nm and PDI 0.276 ± 0.034 , and for BSA adsorbed cationic NPs/NCMPs was 356.73 ± 33.83 nm and PDI 0.467 ± 0.116 , confirming the re-dispersion of NPs from NCMPs after the microcarrier, L-leu, is dissolved.

A scanning electron micrograph (Fig. 1c & d) of the NCMPs revealed the irregular shape and corrugated surface texture. In addition, the size of the NCMPs calculated from the SEM pictures was found to be approximately 2.09 ± 0.16 μ m, based on an average of five SEM images with 60 individual NCMPs in each of them.

The analysis of the thermograms obtained using TGA showed that the dry powder formulation had a residual moisture content of $0.46 \pm 0.01\%$ w/w indicating the drying employed during the SD process was efficient.

3.4. Characterization of BSA and nanoparticle association

Confocal microscopy was used to visualise the association of BSA with NPs. The confocal images (Fig. 2b), reveal that the red and green colours representing NPs and FITC-BSA respectively were present simultaneously, indicating their association. In addition, the increase in particle size observed after adsorption of BSA onto PGA-co-PDL NPs also confirms their association (Table 2).

3.5. In vitro release studies

In vitro release studies were performed on protein adsorbed NPs/NCMPs and reported as cumulative percentage BSA released over time (Fig. 3). An initial burst release, recorded at '0' time point, of $22.45 \pm 2.39\%$ BSA was observed followed by continuous release up to 5 h, with BSA release of $73.74 \pm 6.60\%$. After this time period, a slow continuous release was observed with release of $88.85 \pm 4.38\%$ over 48 h.

Table 1

The average particle size and surface charge of nanoparticles (NPs) prepared using different concentrations of surfactant, DMAB (Mean \pm SD, $n=3$).

Concentration of DMAB (% w/w)	0	1	2
Before centrifugation			
Z-Average size (nm)	162.23 \pm 06.80	175.74 \pm 15.46	128.64 \pm 06.01
Surface charge (mV)	−10.28 \pm 01.00	+13.24 \pm 08.00	+42.32 \pm 02.70
After centrifugation ^a			
Z-Average size (nm)	463.52 \pm 23.69	710.71 \pm 152.66	223.08 \pm 05.60
Surface charge (mV)	−19.14 \pm 01.08	−10.86 \pm 00.84	+35.94 \pm 01.36

The PDI values of all samples were in the range of 0.1–0.2 (before centrifugation) and 0.2–0.3 (after centrifugation).

^a After centrifugation size and charge was determined after two centrifugation runs.

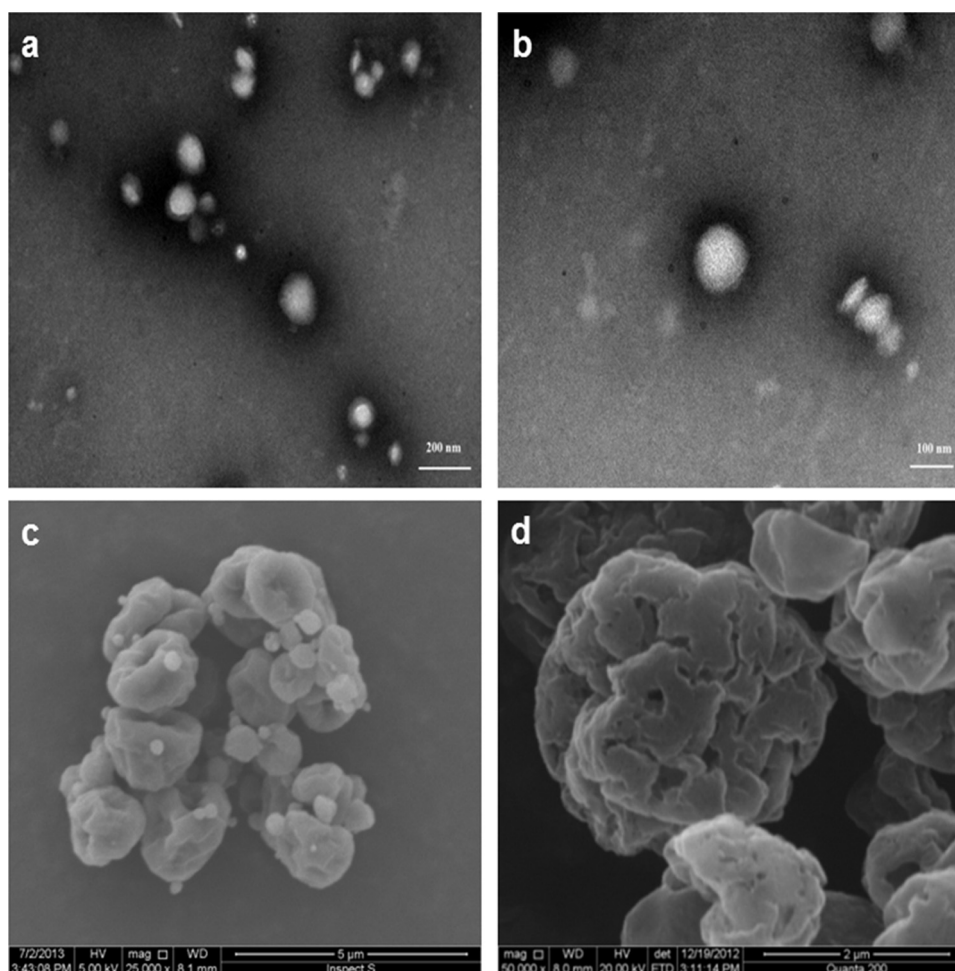


Fig. 1. Transmission electron microscope image of cationic NPs formulated with 2% w/w DMAB stabilizer (a) 44,000X (scale – 200 nm) and (b) 110,000X (scale – 100 nm). Scanning electron microscope images of cationic NPs/NCMPs (c) 5 μ m and (d) 2 μ m.

3.6. Protein stability and activity

The primary structure of BSA released from cationic NPs/NCMPs after 48 h was analysed using SDS-PAGE. As shown in Fig. 4a, standard BSA displays a white band (lane 2) adjacent to the MW standards (lane 1). In addition, the bands for released BSA from cationic NPs/NCMPs (lane 3–5) are identical to that of the standard BSA indicating its stability during and after the SD process.

Conformational changes of BSA released from NPs were determined by CD spectroscopy. The CD spectra of standard BSA and the BSA released are shown in Fig. 4b. As expected, the spectra show minima at 208–210 and 221–222 nm characteristic of α -helical structure. The data for the spectra as presented in Table 3, showed that the predominant structure of BSA was helical displaying 51 and 43% helicity for standard BSA and BSA released, respectively. In addition, the spectral data obtained for standard BSA were in good agreement with previous reports (Norde and Giacomelli, 2000; Zhang et al., 2010).

The esterolytic activity of BSA released from cationic NPs/NCMPs was investigated using 4-nitrophenyl acetate esterase and was calculated to be $78.76 \pm 1.54\%$ relative to standard BSA.

3.7. Aerosol properties of NCMPs

The percentage mass of BSA recovered from the NGI was approximately 83%, well within the pharmacopeial limit of 75–125% of the average delivered dose (2.9.18. Preparations for

Inhalation: Aerodynamic Assessment of Fine Particles., 2010). The deposition data obtained from spray-dried formulations displayed a FPD of $16.57 \pm 0.74 \mu\text{g}$ (per capsule of 12.5 mg), FPF of $70.67 \pm 4.07\%$ and MMAD of $2.80 \pm 0.21 \mu\text{m}$ suggesting that the formulation was capable of delivering efficient BSA to the bronchial-alveolar region of the lungs. The percentage stage wise deposition of BSA in NGI is represented in Fig. 5.

3.8. Cell viability study

The cytotoxicity of cationic NPs and NCMPs was assessed by the MTT assay on A549 cells. The cationic NPs and NCMPs (Fig. 6) indicated a decrease in cell viability with an increase in concentration. The particles showed a cell viability of $74.55 \pm 12.29\%$ (NPs), $95.07 \pm 14.50\%$ (NCMPs) at $78.12 \mu\text{g/ml}$ concentration that reduced to $50.50 \pm 9.41\%$ (NPs), $75.76 \pm 03.55\%$ (NCMPs) at $156.25 \mu\text{g/ml}$ concentration after 24 h exposure. Above $156.25 \mu\text{g/ml}$ concentration, the NPs and NCMPs showed cell survival less than 50%.

4. Discussion

Surfactants are often employed in the NP preparation process to increase the physical stability and decrease agglomeration (Bhardwaj et al., 2009). Herein, the cationic surfactant, DMAB, was employed to prepare positively charged NPs and its use as a surfactant in preparing cationic NPs has been previously reported in the literature (Chen et al., 2010; Hariharan et al., 2006; Kwon

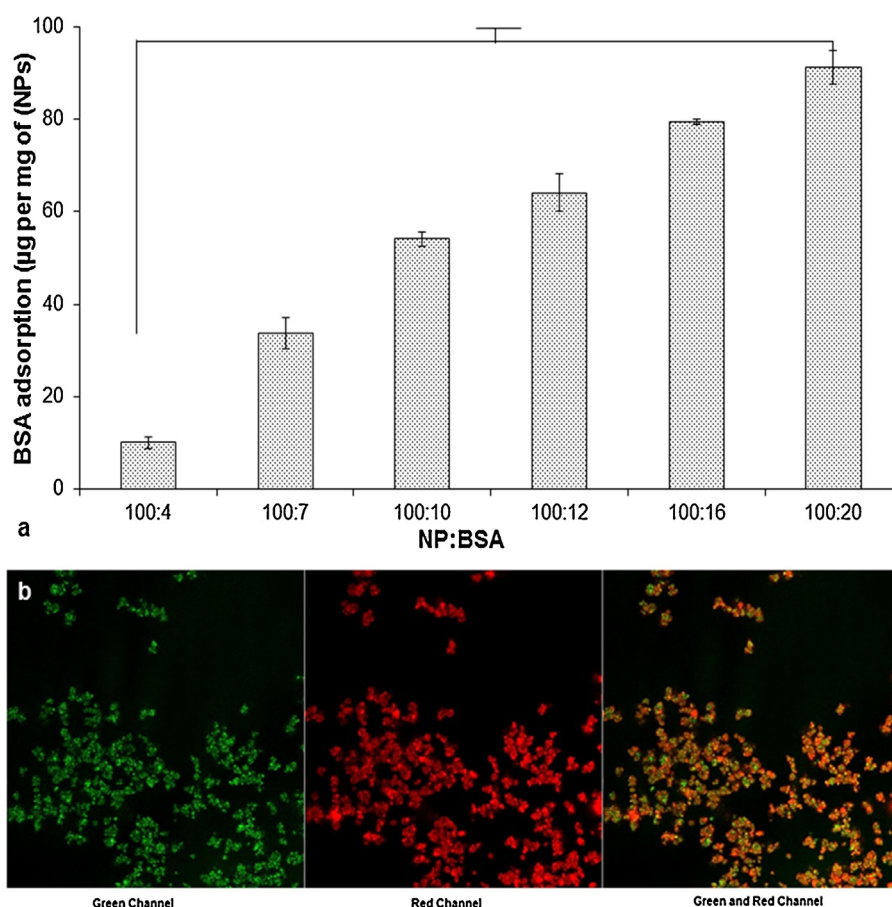


Fig. 2. (a) Amount of BSA adsorbed in µg per mg of nanoparticles (NPs) for different weight ratios of NP:BSA (Mean \pm SD, $n = 3$), (b) Confocal microscopic image, split view, of spray-dried NCMPs containing the fluorescent nanoparticles (red, labeled using Nile red dye) adsorbed with FITC-BSA (green); * $p < 0.05$, ANOVA/Tukey's comparison. (For interpretation of the references to colour in this figure legend, the reader is referred to the web version of this article.)

Table 2

Particle size, PDI and zeta-potential of cationic nanoparticles (NPs) with and without BSA adsorption (Mean \pm SD, $n = 3$).

	NP suspensions ^a	Without BSA adsorption ^b	With BSA adsorption ^c
Particle size (nm)	128.64 \pm 06.01*	234.65 \pm 10.25*	348.36 \pm 14.02*
PDI	0.099 \pm 0.016	0.200 \pm 0.010	0.266 \pm 0.006
Zeta-potential (mV)	+42.32 \pm 02.70	+20.50 \pm 0.17	−01.44 \pm 0.18

a, b and c were subjected to three centrifugation steps, * $p < 0.05$, ANOVA/Tukey's comparison.

^a NPs characterized immediately after preparation without centrifugation.

^b NPs characterized after centrifugation but without adsorption of BSA.

^c NPs characterized after centrifugation and BSA adsorption, 2% cationic surfactant, DMAB, was used for this experiment.

et al., 2001; Mei et al., 2009). In this study, we investigated the effect of surfactant concentration on the particle size and charge of NPs. It was observed that with an increase in the concentration of DMAB, the NP particle size decreased accompanied with an increase in surface charge. The smaller size achieved at the higher concentration of surfactant was due to the broad presence of the surfactant at the o/w interface as reported by Bhardwaj et al. (Bhardwaj et al., 2009). The DMAB concentration of 2% w/w produced positively charged NPs of the smallest size, 128.64 ± 06.01 nm. Similar results showing DMAB altering particle size and surface charge have been reported by others (Bhardwaj et al., 2009; Chen et al., 2010; Hariharan et al., 2006; Kwon et al., 2001). However, after centrifugation the particle size had increased at all cationic surfactant concentrations used accompanied with a decrease in surface charge. This was because of the removal (washing away) of surfactant during the centrifugation process that lead to agglomeration of NPs, due to insufficient covering of

particles. The washing step is necessary so as to ensure the removal of excess or unbound surfactant from NPs (as excessive surfactant can be harmful for delivery). In addition, the washing removed the surfactant coating on the particles resulting in reduced surface charge. Moreover, the NPs (0% DMAB surfactant) have a smaller particle size (463 nm) compared to the 1% DMAB surfactant (710 nm). The reason for this is that the surfactant shown in Table 1 was only cationic DMAB surfactant; however, all the NPs have PVA as an additional surfactant. This may be the reason that we see such a difference in size. The PVA surfactant along with 1% DMAB cationic surfactant is causing some interactions and leading to an increase in particle size of NPs. At 0% DMAB, the PVA is providing some stability and repulsion between particles. However at 1% DMAB there is interaction between +ve DMAB and PVA, hence some particles maybe +ve others −ve after washing, hence the aggregation. At 2% DMAB this dominates the PVA resulting in more stable positive particles.

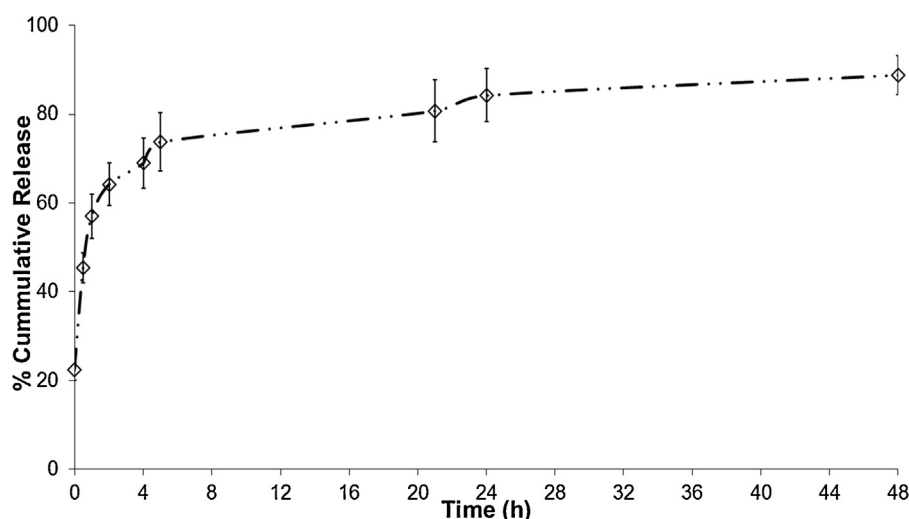


Fig. 3. *In vitro* release profile for BSA from NPs in phosphate buffer saline, pH 7.4 (Mean \pm SD, $n = 3$).

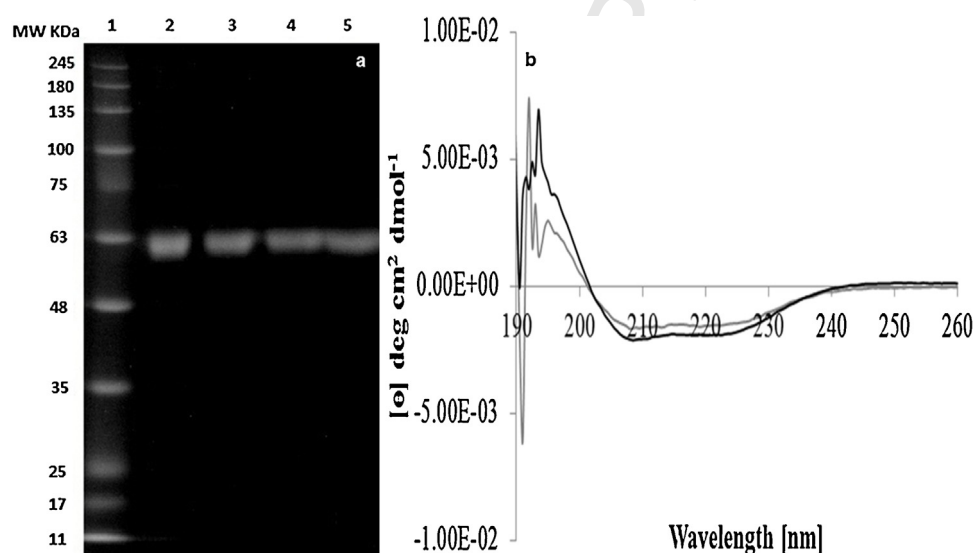


Fig. 4. (a) SDS-PAGE of Lane 1: molecular weight standards, broad range (Bio-Rad Laboratories, Hercules CA, USA), Lane 2: Standard BSA, Lane 3, 4 and 5: Released BSA from cationic NPs/NCMPs after 48 h. (b) CD spectra of standard BSA (black) and BSA released (grey).

Table 3

The percentages of the secondary structures of standard, supernatant and released BSA samples (Mean \pm SD, $n = 3$).

Sample	Helix	Strand	Turns	Unordered
Standard BSA	51.0 \pm 0.007	21.1 \pm 0.070	06.0 \pm 0.010	18.0 \pm 0.007
BSA released	43.0 \pm 0.021	29.5 \pm 0.007	07.0 \pm 0.000	21.0 \pm 0.000

The adsorption of proteins onto polymeric NPs is believed to be dominated by hydrophobic, electrostatic interactions and hydrogen bonding (Yoon et al., 1999). Here, we investigated the effect of BSA adsorption onto the polymeric DMAB-modified cationic NPs wherein the BSA is negatively charged (Regev et al., 2010). The adsorption of BSA onto the cationic NPs increased significantly with an increase in the loading concentration of BSA. This was because more BSA was available for binding and this further suggests the dominance of electrostatic interactions between the BSA and cationic NPs. In addition, the adsorption of BSA onto the surface of cationic NPs was confirmed by an increase in the particle size of NPs after adsorption accompanied with a change in surface

charge from positive to nearly neutral. Once the protein is adsorbed onto the NP, the protein will orientate itself for maximum stability on the surface of the NPs and only expose certain amino acids to the environment resulting in the change in surface charge (Yoon et al., 1999). In addition, the adsorption of BSA was characterized by confocal microscopy which indicated the association of BSA molecules with the cationic NPs. Similarly, Li et al. recently showed that adsorption of negatively charged ovalbumin onto positively charged aluminium hydroxide NPs was mainly driven by electrostatic interactions (Li et al., 2014). Besides, achieving higher adsorption at lower concentrations of added protein, reduces the amount of NPs required to be delivered and for expensive recombinant proteins reduces the amount of initial protein required thereby reducing the cost of the final product.

The NCMPs were produced by SD using L-leu as a microcarrier. The NCMPs containing the cationic NPs had a rough surface and were irregularly shaped. These rough and wrinkled surface characteristics are typical for NCMPs produced using L-leu as an excipient and have been widely reported in the literature (Kunda et al., 2014; Li et al., 2005; Najafabadi et al., 2004; Rabbani and

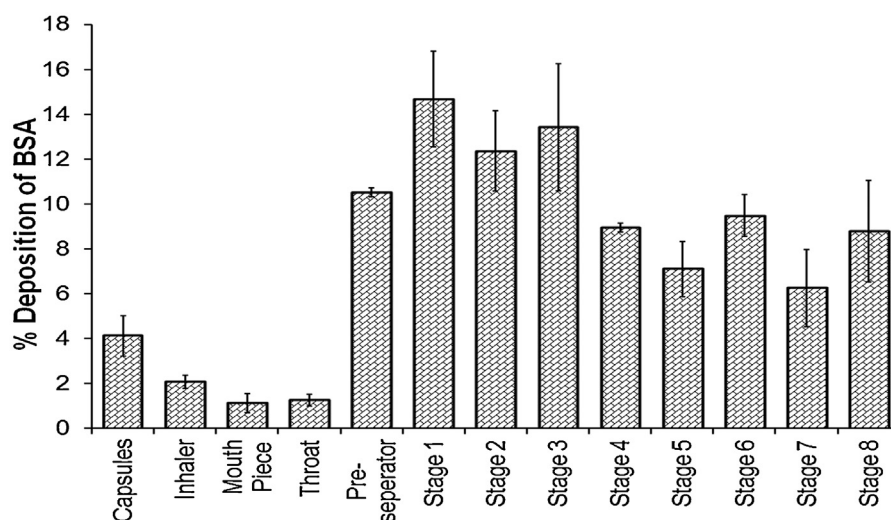


Fig. 5. The percentage deposition of BSA by stage-wise in NGI (Mean ± SD, $n = 3$).

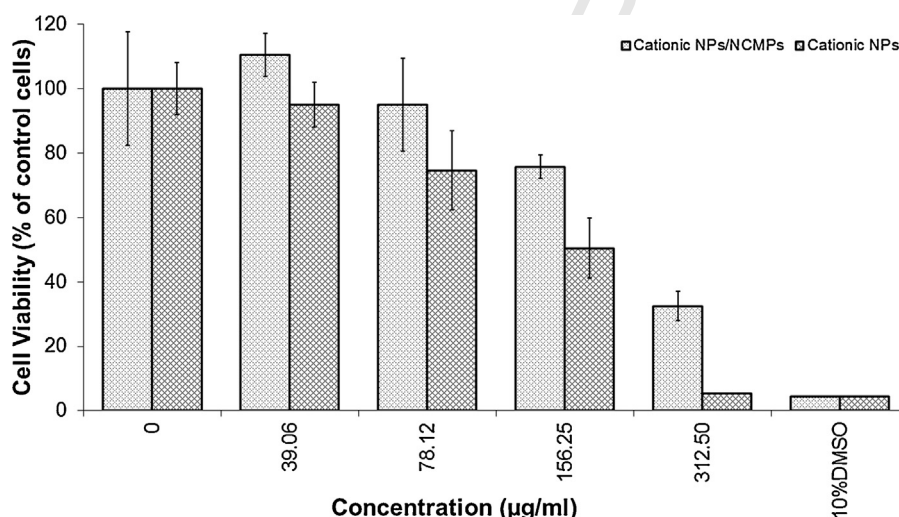


Fig. 6. A549 cell viability measured by MTT assay after 24 h exposure to cationic NPs and NCMPs (Mean ± SD, $n = 3$); Cationic NPs/NCMPs and Cationic NPs.

Seville, 2005; Seville et al., 2007; Sou et al., 2013; Tawfeek et al., 2011; Tawfeek et al., 2013). L-leu is a weak surfactant and it has been established in the literature that L-leu spray-dried particles have a low density are capable of forming a shell thereby encapsulating the particles within (Kunda et al., 2014; Lucas et al., 1999; Najafabadi et al., 2004; Tawfeek et al., 2011; Tawfeek et al., 2013; Vehring, 2008).

The identical bands obtained on SDS-PAGE for standard BSA and released BSA confirmed the stability of protein during the adsorption and SD process. The CD spectral data further confirmed the presence of α -helix (43%) though slightly less than the standard BSA (51%). The slight decrease observed could be due to the adsorption and desorption process of the protein with the NPs. In addition, the released BSA retained ~78% of relative residual esterolytic activity compared to standard BSA. This reduction in activity was expected due to a decrease observed in helicity as determined by CD and could also be because of the adsorption and desorption process of BSA onto NPs. A similar reduction in activity of BSA to 60% when released from hydrogels was observed by Abbate et al. (Abbate et al., 2012).

The aerosol properties of the SD formulation predict an effective delivery to the deep lungs via inhalation. The FPF and

MMAD values suggest an excellent aerosolisation performance and deep lung deposition profile in the bronchial-alveolar region of the lungs (Kunda et al., 2013). The corrugated surface of the NCMPs produced reduces contact points between particles leading to an improved aerosolisation performance (Feng et al., 2011; Sou et al., 2013). The enhanced aerosolisation performance of formulations containing L-leu has been previously reported by others (Li et al., 2005; Najafabadi et al., 2004; Sou et al., 2013).

The residual moisture content in the spray-dried NCMPs formulations induces aggregation and leads to variation in size distribution (Anish et al., 2014). In addition, higher moisture content affects the stability of the formulation and the aerosolisation properties resulting in poor deposition with subsequent reduction of NPs release in the bronchiole-alveolar region. The moisture content obtained here was low (~0.5%) which could be due to the hydrophobicity of L-leu.

The DMAB-modified cationic NPs were relatively toxic at high concentrations; however, the probability of achieving such high local concentrations in the lungs can be excluded as reported by Bhardwaj et al., as the deposited dose would be distributed throughout the lungs (Bhardwaj et al., 2009). One drawback that is often associated with cationic molecules is their cytotoxicity that

limits the dosage to be administered to a minimum thereby resulting in low efficiency (Kwon et al., 2005). Fischer et al. reported that cationic particles made of different polymers, caused toxicity upon interaction with the negatively charged cell membrane surface. Besides, it was also noted that the magnitude of the cytotoxicity of different polymers were highly dependent on the length and concentration of exposure (Fischer et al., 2003). In addition, Harush-Frenkel et al. reported that cationic NPs caused more toxicity compared to anionic NPs (Harush-Frenkel et al., 2008). However, in the case of DMAB-modified cationic PGA-co-PDL NPs, a high adsorption of BSA onto NPs can be achieved thus requiring a low dosage of NCMPs containing cationic NPs to be administered which will address the toxicity concerns. The results obtained above suggest further exploration for use of DMAB-modified cationic PGA-co-PDL NPs for delivery of proteins via inhalation.

5. Conclusions

The DMAB-modified cationic PGA-co-PDL NPs were successfully produced by single emulsion solvent evaporation method. The adsorption of BSA onto the cationic NPs increased with increasing concentrations of BSA due to opposite charges. The BSA adsorbed NPs were successfully spray-dried into NCMPs using L-leu as a microcarrier producing a yield of $48.00 \pm 5.66\%$ with the NCMPs having an irregular and wrinkled surface morphology. The BSA released from the NCMPs was shown to largely maintain its structure under SDS-PAGE and CD analysis with $\sim 78\%$ relative esterolytic activity remaining. Moreover, the FPF of $70.67 \pm 4.07\%$ and MMAD of $2.80 \pm 0.21 \mu\text{m}$ values indicate deep lung deposition in the bronchial-alveolar region. The results obtained above with regards to NP formulation, protein stability and good aerosolisation performance indicate a good potential and encourage more investigation for applications of these materials for pulmonary drug delivery.

References

- Abbate, V., Kong, X., Bansal, S.S., 2012. Photocrosslinked bovine serum albumin hydrogels with partial retention of esterase activity. *Enzyme Microb. Technol.* 50, 130–136.
- Agu, R.U., Ugwoke, M.I., Armand, M., Kinget, R., Verbeke, N., 2001. The lung as a route for systemic delivery of therapeutic proteins and peptides. *Respir. Res.*
- Al-Qadi, S., Grenha, A., Carrión-Recio, D., Seijo, B., Remuñán-López, C., 2012. Microencapsulated chitosan nanoparticles for pulmonary protein delivery: in vivo evaluation of insulin-loaded formulations. *J. Control. Release* 157, 383–390.
- Al-fagih, I.M., Alanazi, F.K., Hutcheon, G.A., Saleem, I., 2011. Recent advances using supercritical fluid techniques for pulmonary administration of macromolecules via dry powder formulations. *Drug Deliv. Lett.* 1, 128–134.
- Anish, C., Upadhyay, A.K., Sehgal, D., Panda, A.K., 2014. Influences of process and formulation parameters on powder flow properties and immunogenicity of spray dried polymer particles entrapping recombinant pneumococcal surface protein A. *Int. J. Pharm.* 466, 198–210.
- Bhardwaj, V., Ankola, D.D., Gupta, S.C., Schneider, M., Lehr, C.-M., Kumar, M.N.V.R., 2009. PLGA nanoparticles stabilized with cationic surfactant: safety studies and application in oral delivery of paclitaxel to treat chemical-induced breast cancer in rat. *Pharm. Res.* 26, 2495–2503.
- Bramwell, V.W., Perrie, Y., 2006. Particulate delivery systems for vaccines: what can we expect? *J. Pharm. Pharmacol.* 58, 717–728.
- Carlotta, M., Di Marzio, L., Rinaldi, F., Carafa, M., Alhaique, F., 2011. Pulmonary delivery: innovative approaches and perspectives. *J. Biomater. Nanobiotechnol.* 2, 567–575.
- Chen, H., Zheng, Y., Tian, G., Tian, Y., Zeng, X., Liu, G., Liu, K., Li, L., Li, Z., Mei, L., Huang, L., 2010. Oral delivery of DMAB-modified docetaxel-loaded PLGA-TPGS nanoparticles for cancer chemotherapy. *Nanoscale Res. Lett.* 6, 4.
- Feng, A.L., Boraey, M.A., Gwin, M.A., Finlay, P.R., Kuehl, P.J., Vehringer, R., 2011. Mechanistic models facilitate efficient development of leucine containing microparticles for pulmonary drug delivery. *Int. J. Pharm.* 409, 156–163.
- Fischer, D., Li, Y., Ahlemeyer, B., Krieglstein, J., Kissel, T., 2003. In vitro cytotoxicity, testing of polycations: influence of polymer structure on cell viability and hemolysis. *Biomaterials* 24, 1121–1131.
- Florindo, H.F., Pandit, S., Gonçalves, L.M.D., Alpar, H.O., Almeida, A.J., 2010. Surface modified polymeric nanoparticles for immunisation against equine strangles. *Int. J. Pharm.* 390, 25–31.
- Greenfield, N.J., 2007. Using circular dichroism spectra to estimate protein secondary structure. *Nat. Protoc.* 1, 2876–2890.
- Hariharan, S., Bhardwaj, V., Bala, I., Sitterberg, J., Bakowsky, U., Ravi Kumar V, M.N., 2006. Design of estradiol loaded PLGA nanoparticulate formulations: a potential oral delivery system for hormone therapy. *Pharm. Res.* 23, 184–195.
- Harush-Frenkel, O., Rozentur, E., Benita, S., Altschuler, Y., 2008. Surface charge of nanoparticles determines their endocytic and transcytotic pathway in polarized MDCK cells. *Biomacromolecules* 9, 435–443.
- Henzler Wildman, K.A., Lee, D.-K., Ramamoorthy, A., 2003. Mechanism of lipid bilayer disruption by the human antimicrobial peptide, LL-37. *Biochemistry* 42, 6545–6558.
- Jiang, W., Gupta, R.K., Deshpande, M.C., Schwendeman, S.P., 2005. Biodegradable poly(lactic-co-glycolic acid) microparticles for injectable delivery of vaccine antigens. *Adv. Drug Deliv. Rev.* 57, 391–410.
- Jiang, M., Wu, Y., He, Y., Nie, J., 2010. Synthesis and characterization of an amphiphilic hyperbranched poly(amine-ester)-co-, -lactide (HPAE-co-PLA) copolymers and their nanoparticles for protein drug delivery. *J. Appl. Polym. Sci.* 117, 1156–1167.
- Kling, J., 2014. Sanofi to propel inhalable insulin Afrezza into market. *Nat. Biotechnol.* 32, 851–852.
- Kumari, A., Yadav, S.K., Yadav, S.C., 2010. Biodegradable polymeric nanoparticles based drug delivery systems. *Colloids Surf. B Biointerf.* 75, 1–18.
- Kunda, N.K., Somavarapu, S., Gordon, S.B., Hutcheon, G.A., Saleem, I.Y., 2013. Nanocarriers targeting dendritic cells for pulmonary vaccine delivery. *Pharm. Res.* 30, 325–341.
- Kunda, N.K., Alfagih, I.M., Dennison, S.R., Tawfeek, H.M., Somavarapu, S., Hutcheon, G.A., Saleem, I.Y., 2014. Bovine serum albumin adsorbed PGA-co-PDL nanocarriers for vaccine delivery via dry powder inhalation. *Pharm. Res.* 1–13.
- Kwon, H.-Y., Lee, J.-Y., Choi, S.-W., Jang, Y., Kim, J.-H., 2001. Preparation of PLGA nanoparticles containing estrogen by emulsification–diffusion method. *Colloids Surf. A Physicochem. Eng. Asp.* 182, 123–130.
- Kwon, Y.J., Standley, S.M., Goh, S.L., Fréchet, J.M.J., 2005. Enhanced antigen presentation and immunostimulation of dendritic cells using acid-degradable cationic nanoparticles. *J. Control. Release* 105, 199–212.
- Li, H.-Y., Seville, P.C., Williamson, I.J., Birchall, J.C., 2005. The use of amino acids to enhance the aerosolisation of spray-dried powders for pulmonary gene therapy. *J. Gene Med.* 7, 343–353.
- Li, X., Aldayel, A.M., Cui, Z., 2014. Aluminum hydroxide nanoparticles show a stronger vaccine adjuvant activity than traditional aluminum hydroxide microparticles. *J. Control. Release* 173, 148–157.
- Lucas, P., Anderson, K., Potter, U., Staniforth, J., 1999. Enhancement of small particle size dry powder aerosol formulations using an ultra low density additive. *Pharm. Res.* 16, 1643–1647.
- Mei, L., Sun, H., Song, C., 2009. Local delivery of modified paclitaxel-loaded poly(ϵ -caprolactone)/pluronic F68 nanoparticles for long-term inhibition of hyperplasia. *J. Pharm. Sci.* 98, 2040–2050.
- Mody, K.T., Popat, A., Mahony, D., Cavallaro, A.S., Yu, C., Mitter, N., 2013. Mesoporous silica nanoparticles as antigen carriers and adjuvants for vaccine delivery. *Nanoscale* 5, 5167–5179.
- Najafabadi, A.R., Gilani, K., Barghi, M., Rafiee-Tehrani, M., 2004. The effect of vehicle on physical properties and aerosolisation behaviour of disodium cromoglycate microparticles spray dried alone or with -leucine. *Int. J. Pharm.* 285, 97–108.
- Norde, W., Giacomelli, C.E., 2000. BSA structural changes during homomolecular exchange between the adsorbed and the dissolved states. *J. Biotechnol.* 79, 259–268.
- Patton, J.S., 1996. Mechanisms of macromolecule absorption by the lungs. *Adv. Drug Deliv. Rev.* 19, 3–36.
- Peetla, C., Labhasetwar, V., 2009. Effect of molecular structure of cationic surfactants on biophysical interactions of surfactant-modified nanoparticles with a model membrane and cellular uptake. *Langmuir* 25, 2369–2377.
- 2.9.18. Preparations for Inhalation: Aerodynamic Assessment of Fine Particles, 2010. European Pharmacopoeia 7.0 Council of Europe, European Directorate for the Quality of Medicines & HealthCare Strasbourg, 274–275.
- Rabbani, N.R., Seville, P.C., 2005. The influence of formulation components on the aerosolisation properties of spray-dried powders. *J. Control. Release* 110, 130–140.
- Regev, O., Khalfin, R., Zussman, E., Cohen, Y., 2010. About the albumin structure in solution and related electro-spinnability issues. *Int. J. Biol. Macromol.* 47, 261–265.
- Scheuch, G., Kohlhaeuff, M.J., Brand, P., Siekmeier, R., 2006. Clinical perspectives on pulmonary systemic and macromolecular delivery. *Adv. Drug Deliv. Rev.* 58, 996–1008.
- Seville, P.C., Learoyd, T.P., Li, H.-Y., Williamson, I.J., Birchall, J.C., 2007. Amino acid-modified spray-dried powders with enhanced aerosolisation properties for pulmonary drug delivery. *Powder Technol.* 178, 40–50.
- Sinsuebpol, C., Chatchawalsaisin, J., Kulvanich, P., 2013. Preparation and in vivo absorption evaluation of spray dried powders containing salmon calcitonin loaded chitosan nanoparticles for pulmonary delivery. *Drug Des. Devel. Ther.* 7, 861–873.
- Sou, T., Kaminskas, L.M., Nguyen, T.-H., Carlberg, R., McIntosh, M.P., Morton V, D.A., 2013. The effect of amino acid excipients on morphology and solid-state properties of multi-component spray-dried formulations for pulmonary delivery of biomacromolecules. *Eur. J. Pharm. Biopharm.* 83, 234–243.
- Stevanovic, M., Uskokovic, D., 2009. Poly(lactide-co-glycolide)-based micro and nanoparticles for the controlled drug delivery of vitamins. *Curr. Nanosci.* 5, 1–14.

- Sullivan, V.J., Mikszta, J.A., Laurent, P., Huang, J., Ford, B., 2006. Noninvasive delivery technologies: respiratory delivery of vaccines. *Expert Opin. Drug Deliv.* 3, 87–95.
- Tawfeek, H., Khidr, S., Samy, E., Ahmed, S., Murphy, M., Mohammed, A., Shabir, A., Hutcheon, G., Saleem, I., 2011. Poly(glycerol adipate-co- ω -pentadecalactone) spray-dried microparticles as sustained release carriers for pulmonary delivery. *Pharm. Res.* 28, 2086–2097.
- Tawfeek, H.M., Evans, A.R., Iftikhar, A., Mohammed, A.R., Shabir, A., Somavarapu, S., Hutcheon, G.A., Saleem, I.Y., 2013. Dry powder inhalation of macromolecules using novel PEG-co-polyester microparticle carriers. *Int. J. Pharm.* 441, 611–619.
- Thompson, C.J., Hansford, D., Higgins, S., Hutcheon, G.A., Rostron, C., Munday, D.L., 2006. Enzymatic synthesis and evaluation of new novel ω -pentadecalactone polymers for the production of biodegradable microspheres. *J. Microencapsul.* 23, 213–226.
- Vehring, R., 2008. Pharmaceutical particle engineering via spray drying. *Pharm. Res.* 25, 999–1022.
- Wendorf, J., Singh, M., Chesko, J., Kazzaz, J., Soewanan, E., Ugozzoli, M., O'Hagan, D., 2006. A practical approach to the use of nanoparticles for vaccine delivery. *J. Pharm. Sci.* 95, 2738–2750.
- Whitmore, L., Wallace, B.A., 2004. DICHROWEB, an online server for protein secondary structure analyses from circular dichroism spectroscopic data. *Nucleic Acids Res.* 32, W668–W673.
- Whitmore, L., Woollett, B., Miles, A.J., Janes, R.W., Wallace, B.A., 2010. The protein circular dichroism data bank, a Web-based site for access to circular dichroism spectroscopic data. *Structure* 18, 1267–1269.
- Yamamoto, H., Kuno, Y., Sugimoto, S., Takeuchi, H., Kawashima, Y., 2005. Surface-modified PLGA nanosphere with chitosan improved pulmonary delivery of calcitonin by mucoadhesion and opening of the intercellular tight junctions. *J. Control. Release* 102, 373–381.
- Yang, W., Peters, J.L., Williams III, R.O., 2008. Inhaled nanoparticles—a current review. *Int. J. Pharm.* 356, 239–247.
- Yoon, J.-Y., Kim, J.-H., Kim, W.-S., 1999. The relationship of interaction forces in the protein adsorption onto polymeric microspheres. *Colloids Surf. A Physicochem. Eng. Asp.* 153, 413–419.
- Zhang, J., Ma, X., Guo, Y., Yang, L., Shen, Q., Wang, H., Ma, Z., 2010. Size-controllable preparation of bovine serum albumin-conjugated PbS nanoparticles. *Mater. Chem. Phys.* 601 (119), 112–117.
- Zhao, L., Seth, A., Wibowo, N., Zhao, C.-X., Mitter, N., Yu, C., Middelberg, A.P.J., 2014. Nanoparticle vaccines. *Vaccine* 32, 327–337.